Metal–Ceramic Adhesion: Quantum Mechanical Modeling of Transition Metal–Al₂O₃ Interfaces

Pere Alemany,[†] R. Samuel Boorse, James M. Burlitch, and Roald Hoffmann*

Department of Chemistry and Material Science Center, Cornell University, Ithaca, New York 14853-1301

Received: October 9, 1992; In Final Form: May 17, 1993

Adhesion of 3d transition metals on the (0001), (10$\bar{1}$0), and (1$\bar{1}$02) surfaces of α-Al₂O₃ is studied using extended Hückel tight-binding band structure calculations. Two main interactions, O–M and Al–M, are found to be responsible for the adhesion strength of the metals to the different faces of the oxide. O–M repulsive closed-shell interactions are a destabilizing factor, while Al–M charge-transfer interactions favor interface formation. From our calculations it seems that coordination of surface aluminum atoms is not especially important in determining the adhesion characteristics of the oxide. The most important factor for adhesion is the ratio of oxygen and aluminum atoms on the surface, which determines the balance between repulsive O–M and attractive Al–M interactions. Adhesion to oxygen-covered surfaces formed under oxidizing conditions may be possible by a charge-transfer mechanism from the metal surface to the partially empty O₂ₚ band.

Introduction

Interfaces between metals and ceramics play a critical role in many materials applications. Metal–ceramic adhesion is important in such diverse industrial areas as microelectronics, catalysts, dentistry, photovoltaic cells, and protective coatings for metals. For instance, in the preparation of heterogeneous catalysts, the nature of the interface is crucial in determining the extent of dispersion of the catalytically active metal on the inactive support. The interactions at the interface in these systems can also play a role in the catalytic activity of the metal, giving rise to the so called strong metal–support interactions (SMSI).[1] The bonding of a metal to a ceramic is also important in the formation of seals between such materials. The integrity of the joints will depend in large part on the physical and chemical interactions at the interface.

Since metal–ceramic adhesion has long been required for a variety of industrial applications, research in this area has been carried out from many different perspectives. Much early work on adhesion was done on liquid metal wetting of oxide ceramics.[2–4] Reaction bonding of metals to ceramics, including metal–ceramic "brazing", has been studied both experimentally and theoretically.[5–7] Experimental studies of the effects of deposition atmospheres on the adhesion of electron-beam evaporated metal overlayers on oxide ceramics have been reported.[8–10] Recently, results on ion beam enhancement of adhesion at metal–ceramic interfaces have been published, as well as some theoretical models to explain these results.[10–12] Studies of the effect of crystallographic orientation of single crystal substrates on metal overlayer adhesion have been conducted.[13] The effects of defects and disorder on interface adhesion have been examined by numerous investigators,[14–18] as have the effects of segregation in metal–ceramic couples.[19–21]

In addition to the experimental work mentioned, studies of the influences on adhesion of atom-to-atom bonding across metal–ceramic interfaces have been carried out with a variety of methods. McDonald, Eberhart, and others provided a rudimentary understanding of adhesion at interfaces with simple phenomenological models and have been able to correctly predict trends in adhesion at metal–sapphire interfaces[4] as well as other simple systems.[22] Recent work by Li has demonstrated the correlation between experimentally obtained work of adhesion values for metal–ceramic couples and the electron density of the metal as well as the thermodynamic stability of the oxide.[23] Charge transfer from the metal to the oxide is seen as important to adhesion in Li's model. The influence of image charges at the interface and the electrostatic factors involved in metal–oxide adhesion have been elucidated by Stoneham and Tasker.[18,24] Investigations of the electronic structure of cluster models[25–35] and more recently of extended systems[36–39] have been carried out for several metal–ceramic interfaces. Results of these calculations have been successfully correlated with experimental results, particularly for metal–ceramic interfaces. The thermodynamics of metal–ceramic interface adhesion has been studied and reviewed by Klomp and others.[6,18,40–42] Other useful approaches to the understanding of metal-ceramic interactions exist, for instance Lee's use of the hard/soft acid–base concepts.[43]

Although much research has been accomplished, the studies and models proposed have not yet provided the ability to predict the correlation between adhesion and the chemical identities of the two partners in metal–ceramic couples. Thus, as recent reviews of the subject point out, there is at present a gap between what can be theoretically modeled and what is practically useful.[7] Further modeling of interfaces is needed to understand and interpret experimental results.[44] To date, no modeling of the effect of dopants in ceramics on metal–ceramic adhesion strength has been done. What's more, no modelling of amorphous metal–ceramic interfaces has been carried out, precluding the possibility of direct application of calculational results to many practical systems of interest.

Electronic Structure of Metal–Ceramic Interfaces

From a chemical point of view, the question of "How do metals adhere to ceramics?" can be rephrased as, "How do two materials with completely different intrinsic chemical bonding characteristics bind to each other?" Quantum mechanical tools have been extensively applied by chemists to answer questions of bonding in molecules and more recently in solid-state problems. It seems, therefore, that the study of complex systems, such as interfaces, by use of quantum mechanical models, could give some insight into the bonding in metal–ceramic adhesion.

Theoretical modeling of metal–ceramic interfaces is especially challenging because of experimental uncertainties or lack of knowledge of interface structures and compositions. Much more is known of systems with interfaces formed by semiconductors such as silicon or GaAs; quantum mechanical studies of interfaces, such as Si(111)/CaF₂[27] or metal–silicon interfaces, have been published in recent years.[45]

From the applications point of view, one of the most important metal–ceramic systems is that consisting of various transition

metals on alumina. Previous modeling of these interfaces has been carried out by Johnson and Pepper[29] (cluster Xα–MO method), by Anderson and co-workers[25,26,28] (cluster ASED-MO method), Kasowski and co-workers[37,38] (ab initio pseudopotential band-structure calculations), and more recently by Kohyama et al.[39] (tight-binding band structure calculations). In these studies different models have been employed to describe the basic features of the interaction between transition metals and the (0001) or $(10\bar{1}0)$ faces of α-Al_2O_3, the effect of yttrium as dopant in Ni on the growth and adhesion of α-Al_2O_3 on Ni,[25] and the influence of interfacial S.[35]

The primary problem encountered when constructing a model for metal–ceramic interfaces is the general lack of available experimental data, especially for large-bandgap insulators as Al_2O_3. Moreover, most of the industrially significant systems, to which much of the experimental work is devoted, are based on amorphous components. Even when some information is available for single-crystal systems, one has to deal with lattice mismatch, incommensurate superposition of lattices, the possibility of surface reconstruction on one or both sides of the interface and defects or disorder in the study of doped systems. In addition to these problems, the size of the systems, with a large number of atoms in the unit cell, often dissuades researchers from using sophisticated quantum chemistry methods for attacking these problems.

In this work we will show that, despite all of the problems encountered in the modeling of metal–ceramic interfaces, there are general trends that can be obtained from simple models. Our aim is to obtain qualitative features of interface bonding and to develop a simple model, based on chemical reasoning, that allows us to gain some insight into the complex phenomena occurring at the interface. The applicability of our theoretical results to real metal–ceramic bonds has to, of course, be taken with caution. The processing methods used for real systems, including high temperatures, can dramatically change the properties and structure of the interface, making direct comparison with our simple models invalid. Our starting point will be the adhesion of first row transition metals to the (0001) face of α-Al_2O_3, since this interface is by far the most studied. We will make qualitative comparisons between our calculational methods and the previously mentioned approaches of Johnson and Pepper[29] and Nath and Anderson.[28] Later we will focus our attention on the variation of interface properties with the existence of ordered vacancies on the (0001) surface of α-Al_2O_3 and with the physically more reasonable Al^{3+} covered (0001) surface. In the last section, the study will be extended to the interactions of the metal surfaces with the $(10\bar{1}0)$ and the $(1\bar{1}02)$ faces of an α-Al_2O_3 single crystal. The problem of doping the ceramic with transition-metal ions (Cr^{3+}) has been addressed in a separate paper.[46]

Modeling of Metal–Ceramic Interfaces

Two main approaches have been used in calculating the electronic structure of extended systems. First, one could assume that all interactions are well-described locally. This leads to a so-called "cluster" model in which the solid is replaced by a finite cluster of atoms, carefully chosen to reproduce all important aspects of the electronic structure of the infinite system. More sophisticated methods embed the cluster in a charge distribution simulating the real solid. The alternative approach is to take advantage of the translational symmetry of the system and apply a reciprocal-space band-theoretic approach.[47,48] In this study we have adopted the second type of approach.

One problem that arises when dealing theoretically with surfaces is their semiinfinite character; surfaces extend in only two dimensions but are finite in the third direction. Mathematically, dealing with infinite systems is much simpler than with semiinfinite systems. The most common resolution is to perform calculations for a two-dimensional infinite slab formed by a finite number of layers.[49] Experience has shown that three-to-four-layer-thick slabs are good enough to mimic the essential

characteristics and differences of bulk and surface layers of the real system.[50] This approach, although conceptually simple, leads to various problems when applied to the modeling of surfaces or interfaces. The first one is the appearance of two surfaces on the slab. In modeling an interface, one of these surfaces will interact with the other component, but the calculations may be perturbed by surface states from the noninteracting surfaces. Such an interaction is clearly an artifact of the model. Surface states of this type appear in large gap insulators as dangling bonds states in the bandgap. Depending on the occupation of these levels, we can have donor or acceptor states that may change the charge-transfer relations across the real interface. To solve this problem one often "passivates" the noninteracting surfaces with the addition of a layer of hydrogen atoms saturating the dangling bonds of the surface.

When one has decided which model to use for the surfaces of both components of an interface, new problems inherent to the modeling of an interface arise. One normally has little or no information on the structure of the interface itself. An important distinction in this respect is the following: Is the interface formed by two pristine surfaces of different materials facing each other at a fixed distance, or is there some immediate region formed by interpenetration of atoms from both species? Assuming the simplest case of two clean surfaces separated by a fixed distance, a great number of questions arise: What is the separation? What is the relative orientation of both surfaces? If both lattices don't fit together, what changes are forced on them by the formation of the interface? To answer each of these questions one often has to introduce somewhat arbitrary assumptions, based either on chemical intuition, or on simplicity. Distances across the interface can be chosen by comparing different compounds involving the atoms present at both sides of the interface. For the relative orientation of both surfaces, one normally assumes the simplest arrangement possible, although in some cases one is forced to study more than one relative orientation for a given system.

The hardest problem is that of lattice mismatch leading to incommensurate interfaces. The approach taken in this work for the alumina–transition metal interfaces, in which the lattice mismatch is not very large, is to change the geometry of one or both materials in such a way that the unit cells become commensurate. We changed the dimensions and the atomic positions of the metallic layers and kept the experimental structure for the α-Al_2O_3 component. This choice is based on the fact that the metal is not as rigid as the oxide and that, for most experimental systems, the metal is being deposited on the exposed face of the ceramic. It then seems reasonable to assume that the arriving metal atoms will adjust their position to the existing "template" ceramic layer.

The last step in modeling an interface is the introduction of specific features of the component in the model. One can try to study the influence of dopants in both materials, of defect states (e.g., vacancies on the surfaces), the effect of reconstruction of the surfaces, or of adsorbed species that may change the adhesion characteristics. It is not easy to introduce these specific features in the models, since they demand either the use of very large unit cells (e.g., for reconstructed surfaces) or of long series of calculations (due to positional disorder, e.g., in doped materials).

Perhaps the most challenging modeling is that of amorphous structures.[51] One possible approach to these complex systems is based on the use of large unit cells that do not exhibit short-range order. These are then periodically repeated to generate an infinite system. One assumes in this approximation that the long-range order effects, due to the periodic boundary conditions, will not introduce important features in the electronic structure of the amorphous compound being modeled. A sufficiently large unit cell can reproduce quite well the electronic structure of the amorphous material modeled.[52] A problem in using this approach in the study of interfaces is the high number of atoms that one needs to reliably model an amorphous interface. Due to the limited capabilities of the calculational programs employed, we have not
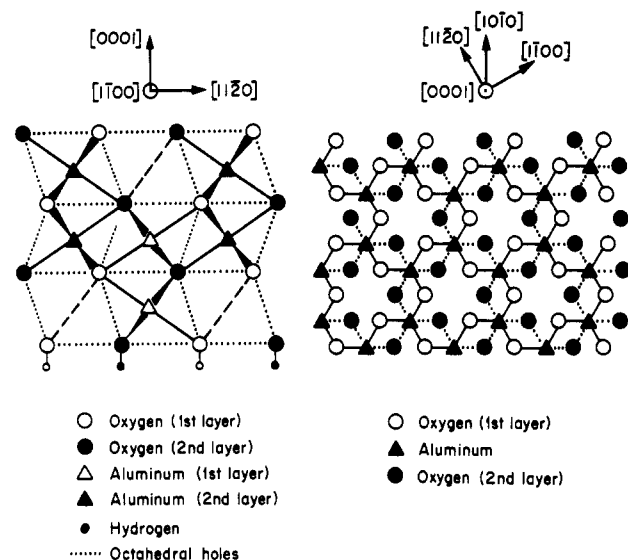
Oxygen (1st layer) ○

Oxygen (2nd layer) ●

Aluminum (1st layer) △

Aluminum (2nd layer) ▲

Hydrogen •

······ Octahedral holes

Oxygen (1st layer) ○

Aluminum ▲

Oxygen (2nd layer) ●

Figure 1. Schematic views of two projections of the corundum structure.

explored amorphous interfaces in our work. A different approach to the modeling of interfaces between amorphous materials is based on the calculation of local densities of states for a cluster embedded in a medium simulating the characteristics of the amorphous material being modeled. One of these methods, the "cluster-Bethe lattice" method,[53] has been applied to the study of the interface between amorphous silicon and SiO_2.[54]

Computational Method

All the calculations presented in this study are of the extended Hückel type.[55,56] Band structures are obtained using the tight-binding approximation.[57,58] More detailed information on the computational method is described in the Appendix. In recent years, this kind of methodology has been successfully applied to the study of bonding in a large number of compounds including molecules, surfaces, and solids.[47,59] Although based on rather crude approximations, the extended Hückel method is especially well suited for extended systems, such as interfaces. This is due mainly to its simplicity, both computationally and conceptually. Extended Hückel calculations should permit us to extract a general qualitative picture of the different bonding interactions across the interface. It is clear that the calculated values of adhesion strength using this method can in no way be taken as a quantitative measure of actual adhesion values. We intend to focus on general trends and changes induced in the interface by varying the metal or the face of the ceramic, to obtain qualitative information of bond strength across the interface, and to establish the chemical basis of the adhesion mechanism between these types of materials.

Adhesion of Transition Metals to the (0001) Face of α-Alumina. The first part of this work is devoted to the study of adhesion of transition metals to the (0001) surface of α-Al_2O_3, by far the most studied face, both experimentally and theoretically. The study of adhesion on this surface allows us to compare our results with those published previously. Our model for the oxide (see Figure 1) consists of three layers of oxygen and aluminium atoms. The experimental bulk geometry of α-Al_2O_3 obtained from X-ray diffraction experiments[60,61] has been used. The surface exposed to the metal is chosen to be an oxygen plane. Recent calculations[62] indicate that this may not be the most favorable cleavage plane and that it is more likely that α-alumina cleaves to give two surfaces with aluminum atoms exposed. Although elementary charge balance arguments make the O^{2-}-covered surface unreasonable, we will start our study with this surface. In a later section we will turn our attention to a more physically reasonable model, based on an Al^{3+}-covered (0001) surface, and analyze its adhesion to metals. Recent work by Rühle and coworkers, using lattice resolved TEM imaging of Nb/(0001) Al_2O_3 interfaces,

TABLE I: Structure, Interacting Faces, and Interlayer Distances (Å) for the Metallic Slabs Used in the Calculations

| M	Sc	Ti	V	Cr	Mn	Fe	Co	Ni	Cu
Struct	hex	hex	bcc	bcc	bcc	bcc	hex	fcc	fcc
face	(0001)	(0001)	(110)	(110)	(110)	(110)	(0001)	(111)	(111)
d_{M-Ox}	2.63	2.34	2.14	2.04	2.18	2.07	2.03	2.03	2.08

indicates that the interfaces studied are clearly *not* Al^{3+} terminated.[63] Most likely, "real" (0001) surfaces have some mixture of Al^{3+} and O^{2-} species.

At the other surface of the slab we add a hydrogen layer to prevent the appearance of unwanted surface states in our calculations. The ratio of aluminum–oxygen layers and metal layers is 1:1. It is important to maintain this ratio when studying the effect of dopants in the ceramic, since the number of charge accepting or donating centers has to be balanced with the number of metal atoms included into the model. The ratio of aluminium to metal atoms is 2/3 for the (0001) surface, 2/5 for the (10$\bar{1}$0) surface, and 1/3 for the (1$\bar{1}$02) surface.

In our calculations we will only use the first row of the transition-metal series. Three-layer slabs have been used as models for the metals. The exposed faces of the metal components selected to interact with α-Al_2O_3 are displayed in Table I, as well as interlayer distances within the metals.[64]

The structure of the layers has been changed slightly so that each metal atom of the interface layer sits on top of one of the oxygen atoms of the α-Al_2O_3 (0001)O surface. The modifications induced on the original metal layer are shown in **1** for the case of chromium.
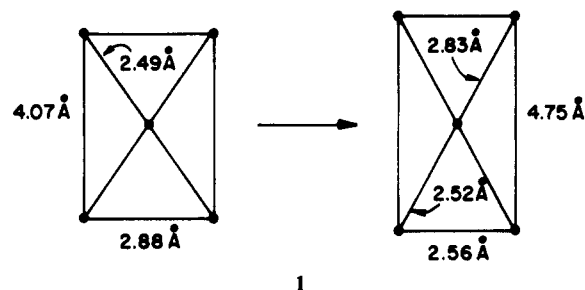
The change affects not only the interatomic distances in the layer but also the symmetry. The stacking pattern of the three layers included in the metal model follows the original structure of the metal. The distance between the alumina and the metal interacting surfaces was fixed in all cases at 2.0 Å (O–metal) in order to simplify comparison of results. No important differences in the basic interactions are expected if this distance were changed within reason. It is not necessary to introduce a "passivation" layer on the noninteracting metal surface since no interfering surface states appear in this case.

The parameters and the sets of special k points used in the calculations are listed in the Appendix. For each interface studied, three separate calculations have been performed: one for the α-Al_2O_3 slab, one for the metal slab, and a third calculation for the composite system. Adhesion energy values are obtained by subtracting the energy of both separated components from the energy obtained for the whole system:

$$E_{adh} = E_{M/Ox} - (E_M + E_{Ox})$$

Negative values for the interface energy (E_{adh}) indicate that the composite is energetically more favorable than the separated slabs.

Electronic Structure of the α-Al_2O_3 (0001)O Surface. Bulk and surface studies of the electronic structure of α-Al_2O_3 have been reported using different methods, both experimental and theoretical. Broad features of the electronic structure are obtained from the results of several optical absorption spectroscopies[65-69] as well as from X-ray emission spectroscopy (XES),[69,70] X-ray photoemission spectroscopy (XPS),[71,72] and electron-energy-loss
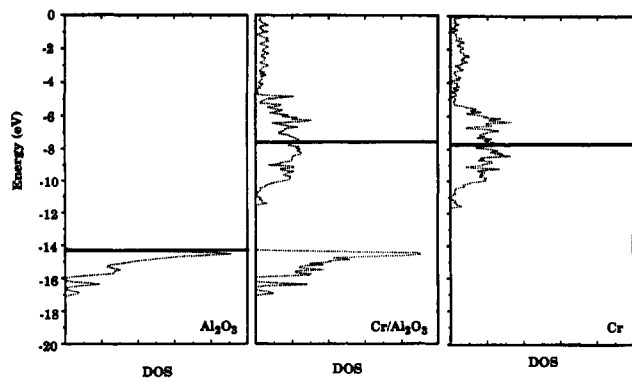
Figure 2. DOS curves for (a) the (0001)O surface of α-Al_2O_3, (b) the α-Al_2O_3–chromium interface, and (c) the chromium (110) surface. The solid bar indicates the position of the Fermi level.

Figure 3. Width of the d band for the transition metal slabs. The dashed line indicates the position of the Fermi level.

spectroscopy (EELS).[73] Theoretically, the electronic structure of bulk α-Al_2O_3 has been examined at semiquantitative[74] or molecular (cluster models)[75-78] levels. Evarestov et al.[79] calculated the energy structure of α-alumina by using the semiempirical Mulliken–Rüdenberg technique. Other studies include those of Batra[80] using the extended tight-binding method, Ciraci and Batra[81] using extended Hückel methodology, Kohyama et al.[39] using a tight-binding Hamiltonian, Causà et al.[82,83] using ab initio Hartree–Fock band structure calculations, and Guo et al.[62,84] using the local-density SCF embedded-cluster method. Ciraci and Batra,[81] Causà et al.,[83] Kohyama et al.,[39] and Guo et al.[62] also study the electronic structure of different surfaces of α-Al_2O_3. These authors, however, use the (0001)Al surface instead of the (0001)O surface. In a later section we will compare our results for the (0001)Al face with the work of these authors.

Our calculations on the (0001)O surface of α-Al_2O_3 (Figure 2a) indicate that its electronic structure is very similar to that of bulk alumina. The valence band is divided into two zones, the lower part (centered around –33 eV, not shown in Figure 2a) is mainly composed of O_{2s} orbitals, while the upper part (centered around –15 eV) is formed by O_{2p} levels. A calculated gap of 14.9 eV (experimental value between 8.0 and 9.9 eV[65,71,73,80,85]) separates this band from the mainly $Al_{s,p}$ hybrid band. The extended Hückel method is known to exaggerate the destabilization of antibonding levels, resulting, in the solid state, in an overestimation of the bandgap in semiconductors and insulators. This problem could be partially solved by using another set of parameters in the calculations. The magnitude of the gap is not essential to the following discussion, so we prefer to use the normal, unadjusted parameters for both Al and O, with which there is much experience. There are no surface states separated in energy from the bulklike bands. The important orbitals for interface formation are thus lone pair (mainly O_{2p}) orbitals located in the region from –16 to –14 eV, their main contribution coming near the top of the O_{2p} band. The coordination of oxygen atoms on the surface of α-Al_2O_3 differs from those in the bulk. While bulk oxygen atoms have a tetrahedral environment formed by four aluminum atoms (two belonging to the layer above and two belonging to the layer below), surface oxygen atoms have lost two of these coordinating atoms. The two remaining lone pairs on these atoms will be involved in interactions with the metal layer.

Electronic Structure for the Transition-Metal Slabs. The electronic structure calculated for the metallic slabs is very similar to that obtained for the bulk metals.[86] A typical density of states plot for a three-layer metallic slab (chromium) is shown in Figure 2c, with the "d band", largely metal 3d, between –12 and –5 eV. Above it is a broad s and p band, the bottom of which substantially penetrates the d band. In fact, at the Fermi level the occupation of the various levels for the atoms of the inner, bulklike, layer is $s^{0.65}p^{0.313}d^{4.38}$, indicating an important filling of the s and p bands. Another important effect extracted from these orbital occupations is that the bulklike inner layer is positively charged (5.34 electrons
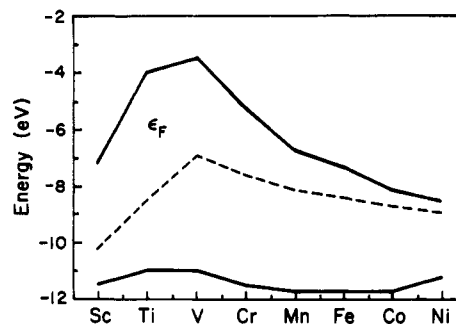
vs the 6 electrons on a neutral chromium atom). Negative charge has accumulated on both surface layers.

To discuss this effect in more general terms,[47] let us analyze what happens on moving from left to right in the transition-metal series. The increased nuclear charge is less completely screened and the d electrons more tightly bound. As a result, the d band comes down in energy while also becoming narrower. At the same time, band filling increases upon moving from left to right in the periodic table. For more detail on this complicated balance, the reader is referred to the work of Andersen.[87,88] These effects are represented graphically in Figure 3. This figure, calculated with extended Hückel parameters later used in the study of adhesion, shows the Fermi level falling as one moves to the right, implying a rise in the work function of the metal. Our results are in qualitative agreement with the results obtained both by experiment and by more sophisticated calculational methods.[86] The Fermi level for copper, not included in the figure, lies higher in energy due to the presence of an electron occupying the s–p band.

Metal–α-Alumina (0001)O Interfaces. In this section we will look at the changes that occur when the metallic and ceramic slabs are joined together. We will examine a specific case, α-Al_2O_3/Cr, and then extend our investigation to the rest of the first-row transition metals.

Our calculations give an interface energy of 0.65 J/m² (corresponding to 0.27 eV/Cr–O pair) for the interface with chromium, indicating that the separated system is energetically favored relative to the interface. This does not mean that it is impossible to have an alumina–chromium interface. We have to remember that we are analyzing the specific interface formed between two faces, the (110) face of bcc chromium and the (0001)O face of α-Al_2O_3. The results apply only for this case and, as will be shown later, can be very different for other interacting faces. We also must be careful not to assign quantitative values to extended Hückel energies. This result is in qualitative agreement with the results of Anderson and co-workers,[25,26,28] who noticed that surfaces perpendicular to the basal plane terminated with O^{2-} or O^- were predicted to adhere very weakly to clean nickel and platinum surfaces. The weak bonding was interpreted by Johnson and Pepper[29] as a donation from low-lying O_{2p} lone-pair orbitals to high-lying metal surface orbitals. According to these authors, the binding energy should decrease with the filling of the high-lying M–O antibonding orbitals. The fact that this interaction is nearly nonbonding is the reason for Nath and Anderson's suggestion that bonding is provided by stabilization of the O_{2s} band of α-Al_2O_3.[28]

Let us now analyze the interactions between both slabs. Looking at the changes in the charges of both systems upon formation of the interface, we can see a net electron transfer of approximately 0.5 electrons from the oxide slab to the metal slab. Most of this charge is transferred from the oxygen atoms of the interacting oxide surface, in complete agreement with Nath and Anderson's observations.[28] The only important difference between our calculation and theirs is the stabilization of the O_{2s} band, which is not apparent in our case. However, as Kohyama et al.[39] point out, there are no experimental data indicating such large
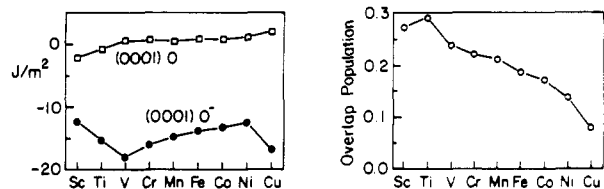
Figure 4. (a) Adhesion energy and (b) interface overlap population for the (0001)O surface. The curve labeled (0001)O⁻ in (a) is for the model with three holes in the O_{2p} band.

changes in the lower valence band of α-Al_2O_3. It also does not seem reasonable that substantial energy changes should occur upon interaction, the metal d and oxygen s orbitals being greatly separated in energy. Analyzing the charges of the metal slab atoms, we find an important electron loss in the exposed metallic surface, although this is compensated by a gain in the bulklike layer.

To obtain an orbital picture of the interactions taking place at the interface, we return to Figure 2. In Figure 2a the DOS of the α-Al_2O_3 (0001)O surface is shown, with its most important peak (the O_{2p} band) at approximately −15 eV. In Figure 2c, we have the DOS curve for the chromium slab, while Figure 2b contains the DOS curve of the total system. Although this is not easily seen from the DOS curves, there is an interaction between both slabs, as a result of which the O_{2p} bands of the oxide layer are slightly lowered, while the metal bands are displaced in the opposite direction. **2** is a schematic representation of the interaction, exaggerated for clarity.

2
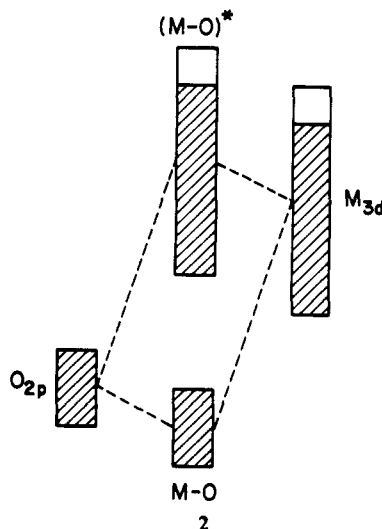
Let us now take a look at the trends in adhesion to the (0001)O face when the transition metal is changed. Figure 4a shows the evolution of the interface energy. The prediction of our model is weak bonding for the first two metals of the series (Sc and Ti) and weakly repulsive interactions for the other metals. Upon moving from scandium to copper, we see a monotonic increase in the repulsive character of the interface. From this trend one may deduce that, independent of the actual values for adhesive strength, failure is more likely to happen for the metals on the right-hand side of the transition-metal series. If we analyze these results with the model shown in **2**, keeping in mind the evolution of band width, band energy, and the Fermi level in the metal slab (Figure 3) when moving from left to right in the periodic table, we may deduce the following facts:

(a) Moving from left to right in the transition-metal series, the d band is lowered in energy, thus giving a better energy match for the interaction. In an orbital interaction, the antibonding combination (the mostly metallic band in our case) is more destabilizied than the bonding combination is stabilized. Since, in our case, the antibonding combinations are partially filled, the greater the interaction, the more the system will be destabilized.

(b) The more we fill the metal band, the more we are filling interfacially antibonding bands, thus decreasing the actual interface bonding strength.

The second effect may be seen in the overlap populations of the oxygen–metal bonds across the interface (Figure 4b). This weakening of interface bonding upon filling of the metal d band has been previously used by Johnson and Pepper[29] to discuss the decrease of adhesion strength in the series Fe, Ni, Cu.

Nath and Anderson[28] propose a model to explain strong adhesion of some metals on the α-Al_2O_3 (0001)O surface. They consider the case when the oxygen atoms in the surface's topmost layer have each lost one electron. The introduction of holes in the O_{2p} band results in strong charge transfer from the surface metal layer to the surface oxygen layer. To compare our results with those published by these authors, we have performed calculations introducing one hole per surface oxygen atom in the O_{2p} band. The adhesion energies calculated for this electron count are displayed in Figure 4a. Our results indicate that adhesion energies are negative, indicating bonding for all the metals used, due mainly to electron transfer from metal to oxide. The strongly bonding adhesion energies obtained are partly due to an overestimation of the charge transfer (ionic contribution) in our one-electron method. They have to be taken with caution. However, it is clear that partial oxidation of the oxygen surface layer leads to better adhesion.

Although our results generally agree with those of Nath and Anderson,[28] there are a few differences worth mentioning. The first difference is related to the nature of our computational method. Band structure calculations do not easily allow the assignment of holes to a particular portion of the structure. Although oxygen surface states lie mostly at the top of the O_{2p} band, contributions from bulk states in this region are very important. In fact, our calculations show that hole occupation is slightly higher for bulk oxygens atoms than for surface ones.

The second point of disagreement with Nath and Anderson's results is in the trends observed in adhesion energies when moving from scandium to copper. While they found monotonically decreasing values for the interface binding energy,[28] our results indicate that this energy (the negative value of the adhesion energy as defined in our model) has a maximum at vanadium, decreasing when moving in both directions (see Figure 4a). At the end of the series, for copper, there is an increase in binding energy, not apparent in the previous results.[28] The trends observed in our calculation are a reflection of the evolution of the Fermi level of the metal slabs when moving from left to right in the periodic table (see Figure 3). The increase in binding energy for copper relative to nickel can be traced to the much higher Fermi level in copper, due to the extra s electron on this element. Our calculations also show, in agreement with Nath and Anderson's model,[28] that it is predominantly the metal surface layer that is oxidized when forming the interface.

The qualitative features of our model are in good agreement with previously published theoretical results and reflect an ability to reproduce the basic aspects of interface formation. In the following sections we will use the results obtained for this interface as a reference for the study of more complex cases. The next step in our plan is to include more details in our basic model of the interface with the (0001) face of α-Al_2O_3. We will start by studying the effect of different oxygen content on the adhesion properties at the interface.

Effect of Different Oxygen Content on the Basal Plane. For basal planes of α-Al_2O_3 terminated with aluminum atoms, coordinatively unsaturated Al^{3+} cations each have an empty sp-hybridized dangling orbital pointing away from the surface. Prior studies of the electronic structure of this surface show that these dangling orbitals form a narrow band low in the O_{2p}–$Al_{3s,p}$ bandgap.[39,62,81,83] Strong bonds to the metal phase are predicted to form between these surface states and the d band of the metal surface. The basic mechanism proposed for the formation of these bonds is donation of charge from the metal surface to the
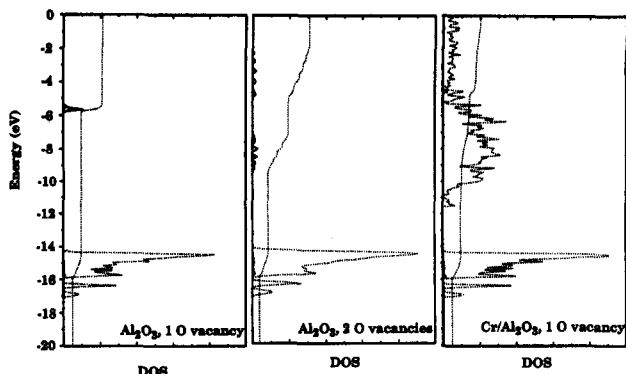
Figure 5. DOS curves for the (0001)O surface of α-Al$_2$O$_3$ with (a) one or (b) two oxygen atoms per unit cell removed from the surface layer, and (c) of the interaction of (a) with chromium.

dangling orbitals of aluminum. Using the results obtained for the (0001)O surface as a starting point, we will study the effect of removal of a different number of oxygen atoms from the initial (0001)O surface. Note that the final (0001) Al surface is obtained by removing the top oxygen layer of the (0001)O surface, and one of the aluminum layers, as shown in 3. Intermediate situations with different O/Al ratios on the surface can be used as models for interface formation under various oxidizing conditions.

3
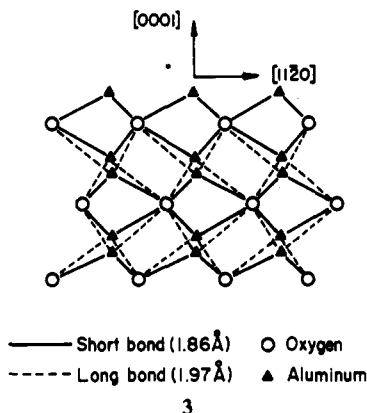
Removal of one or two oxygen atoms per unit cell from the surface layer in our model will produce the vacancy patterns shown in 4. In both cases aluminum atoms, although located in


4
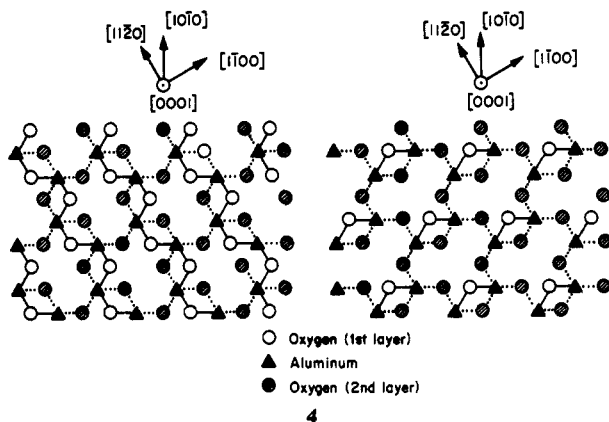
the second and third layers of the slab, are now able to interact directly with the approaching metal slab. Figure 5a,b show the DOS curves calculated for both oxygen deficient surfaces. As expected, in both cases some surface defect bands, from the coordinatively unsaturated aluminum atoms, appear in the O$_{2p}$–Al$_{3s,p}$ bandgap. It is important to consider the oxidation state of the atoms that are being removed. If oxygen is removed as O^{2-} ions, aluminum atoms exposed on the surface will remain as Al^{3+}, giving rise to an empty surface band that can act as an electronic

acceptor. On the other hand, removal of neutral atomic oxygen will result in a reduction of surface aluminum cations, and the now-filled surface band will act as an electron donor. We have studied both electron counts for the models involving partial oxygen coverage of the surface layer, but for the basal (0001)Al plane only Al^{3+} surface cations have been considered.

Figure 6 shows the adhesion energy values calculated for both oxygen-deficient layers. In most cases negative adhesion energy values are obtained, showing that formation of the interface is favorable. Let us start our analysis with two oxygen atoms in the topmost layer. Figure 5c shows the interaction of the surface states with the metal layer. Although difficult to see from the DOS curve, the interaction can be clearly detected from a comparison of the integrated density of states (IDOS) curves for the surface states before (Figure 5a) and after (Figure 5c) interaction. The step at approximately –6 eV, present in the IDOS curve before interaction, disappears, giving place to a gradual increase of the IDOS for the interacting system in the region –8 to –4.5 eV, and a smaller step at this last energy value. This reflects the splitting of the original defect band into two bands, a lower metal–ceramic bonding band and an upper metal-ceramic antibonding band.

To assess the effect of the interaction on the adhesion energy it is necessary to know the relative position of the surface band with respect to the Fermi level of the metal. The trends shown by the adhesion energy curves in Figure 6 are caused by vacancy levels lying above the Fermi level for all metals. If the vacancy band is empty, the adhesion energy should follow the trend found for the (0001)O surface. The effect of interaction 5 will be that of providing some additional stabilization. We now obtain stable interfaces for scandium to manganese, while for the (0001)O surface almost all interfaces were predicted to be unstable.

5
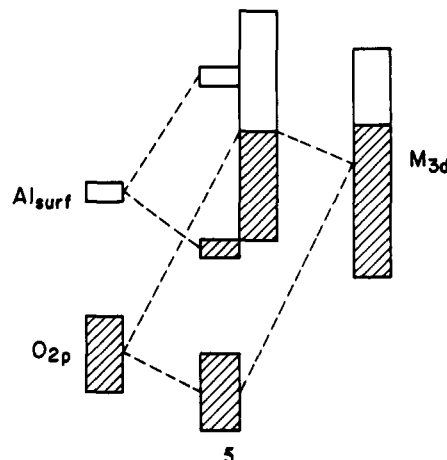
The trend is the same, differing only in the additional stabilization energy provided by interaction with the vacancy. The magnitude of the interaction term is, of course, not constant for the whole series, depending on the overlap and energy match between the surface aluminum levels and the metal surface layer. The magnitude of the interaction energy can be roughly estimated from the difference in adhesion energies for the (0001)O surface and the surface with oxygen vacancies. The interaction energy is found to be on the average approximately 0.5 J/m^2.

On the other hand, when the vacancy states are considered to be full (this means that both aluminum atoms in the second and third layers are considered as Al^{2+}), the variation of adhesion energy with the metal is quite different. The shape of the adhesion energy curve (Figure 6) is dictated by charge transfer from vacancy states to the metal. The adhesion energy curve thus reflects variation of the Fermi level for different metal slabs. In all cases negative values for the adhesion energy are obtained. The most favorable case is scandium, where the energy difference between the vacancy states and the Fermi level is large, and where the almost empty metal band acts as a good electron acceptor. The
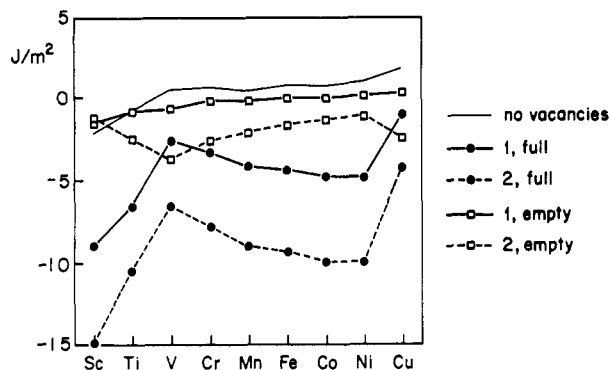
Figure 6. Adhesion energies for the oxygen deficient (0001)O surfaces with filled and empty vacancy states. Numbers 1 and 2 refer to number of missing oxygen atoms on the surface. The top line indicates the adhesion energy for the original (0001)O surface.

Figure 7. DOS curves for (a) the (0001)Al surface of α-Al$_2$O$_3$, (b) the α-Al$_2$O$_3$–chromium interface, and (c) the chromium (110) surface.

adhesion energy decreases in magnitude for titanium and vanadium and increases again on moving from chromium to nickel. The totally filled d band and the extra s electron in copper are responsible for the sharp decrease in adhesion energy calculated for this metal. Most of the stabilization energy obtained in this case is due to electron transfer from the metal to the empty surface states (ionic contribution). The rest is due to covalent interaction provided by the partially exposed aluminum atoms on the oxide slab. The results must be taken with some caution due to the overestimation of charge transfer, and hence of the ionic term in the adhesion, in our one-electron method.[89] Nevertheless, the general piciture of the adhesion mechanism remains valid.

The case of two oxygen vacancies on the surface can be analyzed in similar terms. Here (Figure 5b) the surface vacancies form two bands, extending from -9.5 to -7 eV and from -5 to -2 eV. The lower band is in the energy region where the Fermi level is located for almost all metal slabs. With empty surface states we will have two competing phenomena: stabilization of the interface by interaction of the metal slab with the surface band (covalent term), and the electron-accepting nature of the surface band (ionic term). The adhesion energy curve (Figure 6) is basically the mirror image of the Fermi level curve of the metal slabs, indicating that the mechanism of interface formation in this case is based on the metal acting as a donor to the empty states of the surface. This can be corroborated by taking a look at the charges of the metal atoms before and after the interaction. On average, 0.15 electrons/metal atom are donated by the metal slab, except for scandium where the lower surface band of the oxide is located over the Fermi level of the metallic slab. Both the covalent term and the ionic term lead to charge donation from the metal to the aluminum atoms on the oxide surface, and it is difficult to separate the contributions.

When all surface states are considered to be filled (removal of two neutral oxygen atoms from the (0001)O surface) the situation is very similar to the one obtained for one oxygen vacancy with the surface band being occupied. The main stabilization mechanism is provided by donation of electrons in high-lying surface bands to the metal slab. Of course, we cannot neglect the contribution to the adhesion energy of the interaction of the surface bands with the metal. This interaction can be destabilizing, especially for nearly filled bands. This effect is analogous to the two orbital–four electron destabilizing interactions found in discrete molecules.[59] Although two oxygen atoms have been removed from the surface, no important changes in adhesion energy are found relative to the previous case, where we had only one oxygen atom missing. This can be attributed to the relatively long distance separating the metallic slab from the aluminum atoms (2.84 and 3.33 Å), which prevents strong Al–metal interactions. The differences observed with full Al–surface bands are due only to the larger number of electrons that can be transferred in the case of two oxygen vacancies. The possible movement of one of the metal atoms in the first layer into the
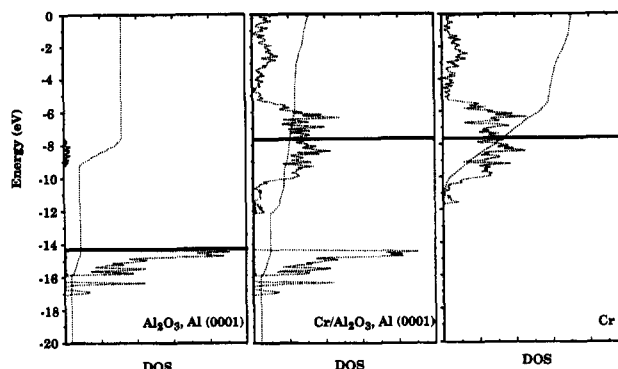
hole left by the oxygen vacancy is calculated to be energetically unfavorable (calculations have been performed only for chromium slabs). The gain in bonding interactions with the exposed aluminum atoms is not enough to compensate for the loss in bonding with the adjacent metal atoms on the slab.

The most interesting case of the series is the (0001)Al surface. There is experimental evidence for the existence of this surface.[90–94] This surface has been shown to be stable and unreconstructed up to approximately 1250 °C. At higher temperatures a weakly reconstructed ($\sqrt{3} \times \sqrt{3}$)R30° surface appears, leading to a stable ($\sqrt{31} \times \sqrt{31}$)R9° structure upon further heating. This reconstruction is stable up to 1700 °C. French and Somorjai[90] have given a possible explanation of the appearance of the large surface unit cell based on the formation of an AlO cubic surface layer by oxygen loss. In the process aluminum atoms have been reduced from their original Al^{3+} state to Al^{2+}.

We will focus only on the low temperature (0001)Al bulklike surface. The fact that this surface is stable up to 1250 °C makes it a good model for metal–ceramic adhesion samples prepared with α-Al$_2$O$_3$ in relatively low-temperature conditions in the absence of atmospheric oxygen. Figure 7a shows the DOS curve for the pure (0001)Al surface. Our calculations give a narrow surface band located in the region -9 to -8 eV. The band is mainly composed of 3s and 3p surface aluminum orbitals. These results are in good qualitative agreement with those obtained by other authors using different computational methods.[62,81,83]

If we look at the effects of interaction of this band with the metal slab (Figure 7b), we see that the DOS of the surface states is now spread over the region -12 to 0 eV, indicating strong Al–M interaction. This interaction, together with some charge transfer contribution, results in the formation of strong Al–M bonds. The number of electrons accepted by the surface aluminum atoms (Figure 8b) follows the same trend as the Fermi level of the metal slab, with maximum electron transfer for vanadium. The values obtained in our calculations agree in magnitude with the 0.79 electron transfer obtained by Anderson et al.[26] in their study of the (0001)Al–Pt interface, although the geometry of their interface is slightly different from ours. While surface aluminum atoms are kept on top of the metal atoms in their model, in our case, aluminum atoms are positioned in 3-fold hollows of the metal layer.

The magnitude of charge transfer to the surface Al^{3+} sites also determines the strength of the interface, as shown from the adhesion values in Figure 8a. The more electrons transferred, the more stable the resulting interface. A comparison of our values with those obtained by Anderson et al.[26] (3.7 eV per surface Al for the Pt//α-Al$_2$O$_3$ system) shows that both methods basically agree in the description of the interactions at the interface. A more detailed study of the interface formation shows that the interface overlap population, Figure 9a, (overlap population between the Al^{3+} sites on the oxide surface and the three closest metal atoms on the metal surface) increases to a maximum at vanadium, and then decreases until nickel. The interface formed with copper is stronger than with chromium, in clear disagreement
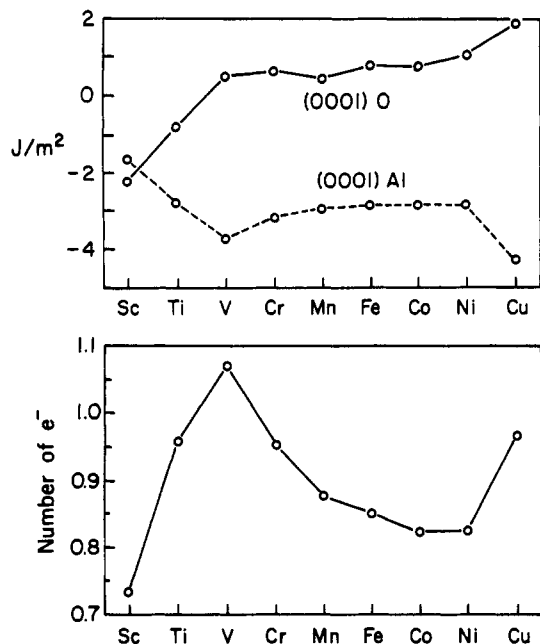
Figure 8. (a) Adhesion energy and (b) charge on the surface aluminum atoms for the interfaces formed with the (0001)Al surface.
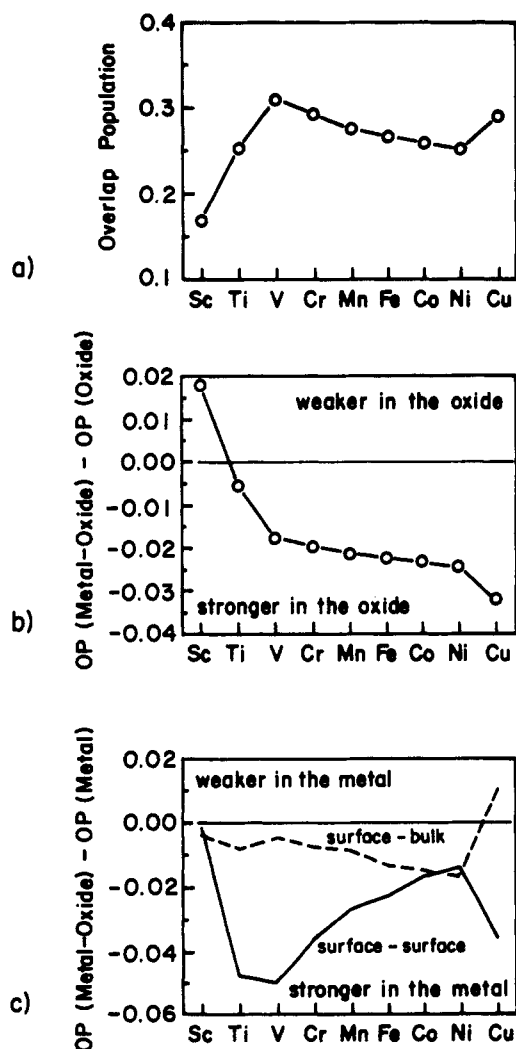

Figure 9. (a) Aluminum–metal overlap populations for the interface with the (0001)Al surface (b) changes in overlap population upon formation of the interface for the oxide and (c) the metals.

with the experimental results which indicate that chromium adheres better to α-Al_2O_3 than copper.[95] The increase in adhesion energy and interface overlap population in the case of copper is produced by the extra s electron present in this metal. This

electron is located in a relatively high-lying s band and contributes greatly to the adhesion energy by the charge-transfer mechanism which, as stated earlier, is greatly overestimated by our method of calculation. In the case of chromium, although the Fermi level of the isolated metal slab lies slightly higher than the vacancy state, the covalent term provides the major part of the stabilization energy, thus giving a more reliable value for the adhesion energy.

Examination of bond strength changes upon formation of the interface (Figure 9b) shows a general weakening of the Al–O bonds between the surface Al atoms and the first oxygen layer of the slab. This weakening increases on moving from left to right in the transition metal series, copper producing the greatest weakening in the oxide. These results indicate that adhesion failure in Cu/α-Al_2O_3 pairs could be related to failure in the oxide and not at the interface itself. To see the effect of interface formation on the metal slab we can look at the overlap population between metal atoms in the surface layer and metal atoms in the second layer (Figure 9c). Formation of the interface weakens the metal bonds on the surface layer, an effect contrary to that obtained for interaction with the (0001)O surface. Bonding between the surface and the first bulk layer is weakened in all cases except copper. The magnitude of the weakening is, in general, larger for the bonds between surface atoms. This weakening is produced by admixture of surface Al orbitals in the metal bands; the mixing has the effect of forming Al–M bonds. at the expense of M–M and Al–O bonding in both components. Interaction of Al is mainly with the surface layer of the metal (overlap between surface aluminum cations and second layer metals is negligible). This results in substantial mixing of aluminum states into the surface band, and thus in an important weakening of surface–surface bonds. The bulklike bands of the metal remain practically unchanged.

Interfaces Formed with Other α-Al_2O_3 Surfaces. In the previous sections we have studied adhesion of transition metals to the basal plane of α-Al_2O_3. While some experimental research has been published on adhesion of metals to other faces of corundum, little theoretical work has been performed for these systems. The two surfaces on which we will focus our attention here are the $(10\bar{1}0)$ face and the $(1\bar{1}02)$ face. The first surface is parallel to one of the prismatic planes and has been used by Morozumi et al.[96] in a study of Nb/Al_2O_3 interfaces. Some theoretical work has been devoted to the electronic structure of the bare surface[83] as well as adhesion of copper to this face.[36,38] The $(1\bar{1}02)$ surface has been employed by Gillet et al.[97,98] to study the formation of Pd/Al_2O_3 interfaces. The electronic structure of the $(1\bar{1}02)$ surface has been studied both experimentally[99] and theoretically.[62]

The two faces of α-Al_2O_3 give surfaces with both oxygen and aluminum atoms exposed. The latter are not fully coordinated and produce dangling bond states appearing in the bandgap of the bulk α-Al_2O_3 band structure. It is precisely the presence of these surface bands that makes the study of metal adhesion on these faces interesting. Size limitations in our band-structure program forced us to use a single monolayer of metal atoms to model the metal surface. Although this is not desirable, most of the interactions between the metal surface and the ceramic are still present in this model. The results have to be analyzed with special care to rule out undesirable effects due to the poor description of the metal surface.

Adhesion on the $(10\bar{1}0)$ Surface of α-Alumina. Figure 10 shows two different views of the slab used to model the metal–ceramic interface for the $(10\bar{1}0)$ surface of α-Al_2O_3. The surface employed in this paper differs from that used by Causa et al.[83] These authors appear to use an O^{2-}-covered surface while, in our model, a nonpolar surface plane, with both O^{2-} and Al^{3+} ions exposed, has been considered. We can see that the aluminum atoms on the surface are 4-fold coordinated. The metal layer geometry is slightly changed from the one used in the previous sections in order to fit the dimensions of the oxide surface. The unit cell contains 10 metal atoms in two rows. As can be seen from Figure 10, metal atoms interact with different atoms on the oxide surface.
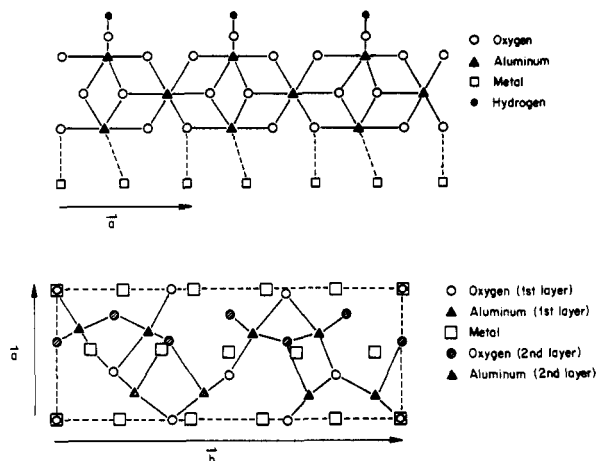
○ Oxygen
▲ Aluminum
□ Metal
● Hydrogen

○ Oxygen (1st layer)
▲ Aluminum (1st layer)
□ Metal
◑ Oxygen (2nd layer)
▲ Aluminum (2nd layer)

Figure 10. Schematic views of two projections for the (10Ī0) surface of α-alumina.

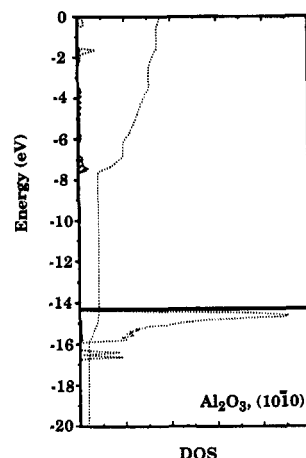**Figure 11.** Density of states for the (10Ī0) surface.

While there are some atoms which lie almost directly on top of oxygen atoms, others lie close to a single aluminum atom or close to both an aluminum and an oxygen atom. Still others do not have any close contact with the surface. This makes the analysis of interactions across the interface extremely difficult. When considering charges on the metal atoms we will refer to the average value obtained for the whole layer, while the interface overlap populations will be divided into two different terms: Al–M interactions and O–M interactions, obtained by averaging values for interactions of each type present at the interface.

The density of states for the α-Al₂O₃ (10Ī0) surface is displayed in Figure 11. As expected, we observe the presence of surface bands due to coordinatively unsaturated aluminum atoms on the surface. Our results are in qualitative agreement with those obtained by Causà et al.[83] using Hartree–Fock band structure calculations. As these authors pointed out, these states form a relatively broad band because surface aluminum ions are arranged in chains, while on the basal planes they are isolated from each other.

Examination of the values obtained for the adhesion energy for this surface (Figure 12) shows a trend very similar to that calculated for the (0001)Al surface. The basic mechanism for adhesion, thus, is related to the formation of strong Al–M bonds with the surface Al states acting as electron acceptors. As in the (0001)Al case, the best adhesion energy values correspond to the most effective charge transfer from the metal surface to the aluminum atoms at the oxide surface. A good adhesion energy for copper is obtained, although this result should be considered with caution for the reasons mentioned above. Adhesion energies are smaller for the (10Ī0) surface, indicating the coexistence of stabilizing Al–M interactions with repulsive Al–O interactions. Half of the metal atoms lie quite far from the nearest surface
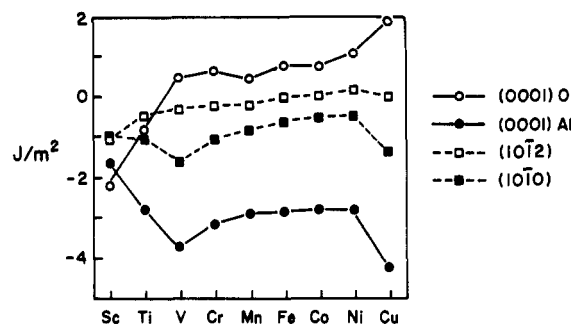

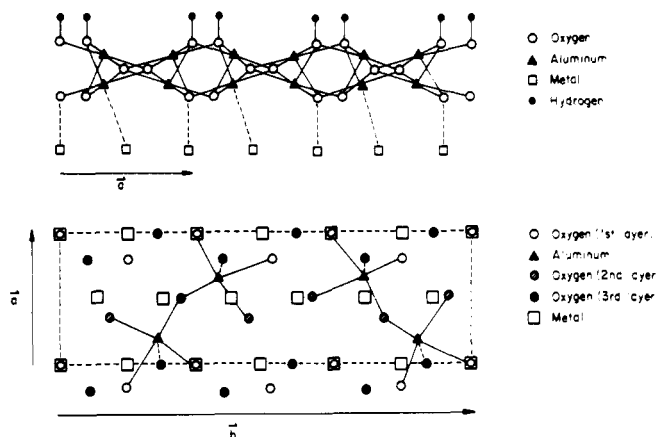**Figure 12.** Adhesion energies for the interfaces formed by the different α-alumina surfaces.

○ Oxygen
▲ Aluminum
□ Metal
● Hydrogen

○ Oxygen (1st layer)
▲ Aluminum
◑ Oxygen (2nd layer)
● Oxygen (3rd layer)
□ Metal

Figure 13. Schematic views of two projections for the (1Ī02) surface of α-alumina.

aluminum site, allowing only unfavorable interaction with surface oxygen atoms.

Examination of the interfacial overlap populations (Al–M and O–M) shows that, although different in magnitude, the trends exhibited on changing the metal layer are the same as were found for the (0001)Al and (0001)O cases, indicating a competition between both types of interactions.

(1Ī02) Surface. Figure 13 shows two different views of the slab used to model the (1Ī02) surface. It has a layer of 3-fold coordinated oxygens on the surface, each with a lone-pair dangling orbital pointing outside the surface. The second layer is formed by aluminum atoms coordinated by five oxygen atoms, two of them in the surface layer, two from the third layer, and the last one located on the fifth layer. The appearance of some surface states in the bandgap of the bulk band structure is expected. Terminating the slab's back oxygen layer with hydrogen atoms is sufficient to obtain bulklike charges for the aluminum atoms on the back surface. The position of the metal atoms at the interface is also shown in Figure 13. We expect the adhesion energy to be dominated by repulsive M–O interactions, although some stabilization could be provided by interaction with the partially exposed aluminum atoms on the second layer.

Figure 14 shows the calculated DOS for the bare α-Al₂O₃ (1Ī02) surface slab. Some high lying surface states appear in the bandgap as expected. The widths of these bands are smaller than those of the (10Ī0) surface, due to the isolated character of the surface Al atoms.

The adhesion energy values calculated for this system (Figure 12) are relatively small, but for all metals from scandium to iron the formation of the interface is favorable. The trend observed is similar to the behavior exhibited by the (0001)O interfaces, showing an important contribution to the overall energy of the repulsive M–O interactions. Stabilization of the interface is provided to some extent by Al–M interactions. Figure 15 shows the change in the number of electrons on the metal atoms when forming the interface. Metal atoms located on top of oxygen atoms of the first layer (metal atoms on the edge of the unit cell,
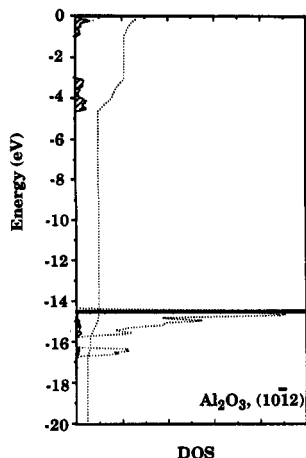
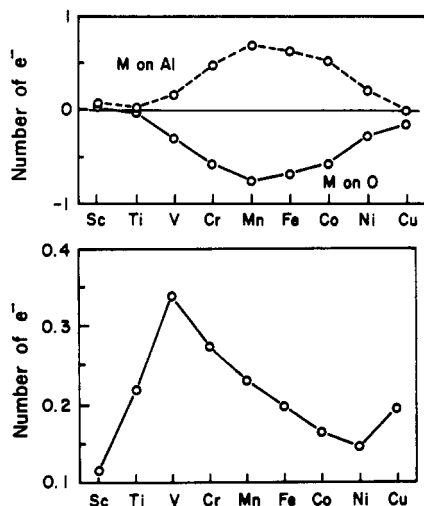**Figure 14.** Density of states for the $(1\bar{1}02)$ (= $10\bar{1}2$) surface.


Figure 15. Changes in charge upon formation of the interface with the $(1\bar{1}02)$ surface for (a) the metal atoms and (b) the exposed aluminum atoms.

see Figure 13) lose charge when forming the interface. Meanwhile metal atoms located on the center of the unit cell act as electron acceptors, gaining almost the same number of electrons as those lost by the adjacent row of metal atoms. In this case electrons flow in the opposite direction, as would be predicted intuitively: metal atoms in the middle row can interact with empty aluminum surface bands, reducing the surface aluminum cations.

An interaction diagram for both metal rows, **6**, shows that interaction of one row with oxygen atoms on the oxide results in destabilization of the metal d band. For the other row, interaction
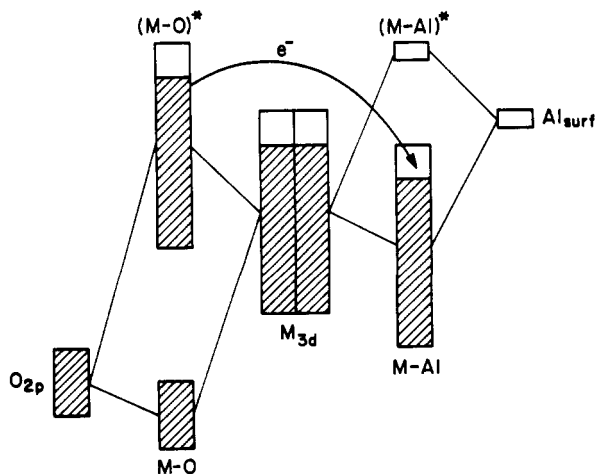
with empty aluminum surface states stabilizes the d band. The

net result is an indirect electron flow from the higher lying metal band to the lower one. Participation of Al–M in the interface formation process can be easily confirmed by the charge accepted by the aluminum atoms, as shown in Figure 15b. **6** also provides an explanation of the adhesion energy decrease with electron filling of the d band. For the last elements in the transition-metal row the indirect electron flow produced by both interactions is not very effective, due to the inability of filled metal bands to accommodate electrons.

The adhesion energy has been measured for this surface for the case of Pd. If we compare the value obtained by Gillet et al.[98] (-1.1 J/m^2) with the value obtained in our calculations for nickel (0.2 J/m^2), we find an important disagreement: our interface is predicted to be unstable.

Important effects on the adhesion energy are expected from the oxygen vacancies described in the experimental work by Gillet et al.[98] Unfortunately the large unit cell necessary for a model that would include the proposed oxygen vacancies makes this system (one of the few with a relatively well-studied interfacial structure) unreachable with our computing resources. From the effects of oxygen vacancies on the (0001)O surface we can nevertheless deduce that the existence of O vacancies on the surface would have the effect of increasing the strength of the metal–ceramic interface.

Conclusions

In this work we have employed the extended Hückel approximate molecular orbital method to analyze factors affecting transition-metal adhesion to different faces of α-Al$_2$O$_3$. Despite the simplicity of the electronic structure calculations employed for this purpose, some basic conclusions can be reached. Two different interactions determine the adhesive properties of α-Al$_2$O$_3$. On one hand, surface oxygen atoms engage in a repulsive interaction with the metal atoms. This repulsion is especially important for the late transition metals, where the almost filled d bands result in high energy, destabilizing M–O antibonding orbitals at the interface. Surface aluminum atoms, providing dangling bond states located in the bandgap of the bulk material, seem to be responsible for the adhesion. The basic mechanism of adhesion is the formation of strong aluminum–metal bonds in which surface aluminum atoms act as electron acceptors. Some part of the stabilization energy is due to ionic contributions, that is, charge transfer from the metal to the surface aluminum atoms. From our calculations it seems that coordination of surface aluminum atoms is not especially important in determining adhesion characteristics of the oxide. In our studies the most important factor for adhesion is the ratio of the oxygen and aluminum atoms on the surface, which determines the balance between repulsive O–M and attractive Al–M interactions. These conclusions hold for only the simple model involving Al^{3+} and O^{2-} ions on the oxide surfaces.

An alternative mechanism for reducing the effect of repulsive O–M interactions is the formation of an interface with partially oxidized oxygen anions (O$^-$). Charge transfer from the metal to these anions provides a strong contribution to interfacial bonding. More elaborate models than ours are necessary to properly describe the interfaces formed by partially oxidized or reduced surfaces. This study provides some potentially useful insights about the chemical aspects of the adhesion between metals and α-Al$_2$O$_3$. This description will serve as a basis for further theoretical work, using a better description of the electronic structure and expanding the results to other industrially important metal–ceramic couples involving AlN or γ-Al$_2$O$_3$.

TABLE II: Extended Hückel Parameters

atom	orbital	H_{ii} (eV)	ξ_1	ξ_2	c_1	c_2
Al[101]	3s	−12.30	1.17			
	3p	−6.50	1.17			
O[56]	2s	−32.30	2.28			
	2p	−14.80	2.28			
Sc	4s	−5.70	1.30			
	4p	−2.94	1.30			
	3d	−9.50	4.35	1.70	0.4228	0.7276
Ti	4s	−6.30	1.50			
	4p	−3.20	1.50			
	3d	−8.00	4.55	1.40	0.4206	0.7839
V[50]	4s	−6.70	1.60			
	4p	−3.40	1.60			
	3d	−6.70	4.75	1.50	0.4560	0.7520
Cr[50]	4s	−7.30	1.70			
	4p	−3.60	1.70			
	3d	−7.90	4.95	1.60	0.4876	0.7205
Mn[50]	4s	−7.50	1.80			
	4p	−3.80	1.80			
	3d	−8.70	5.15	1.70	0.5140	0.6930
Fe[50]	4s	−7.60	1.90			
	4p	−3.80	1.90			
	3d	−9.20	5.35	1.80	0.5366	0.6678
Co[50]	4s	−7.80	2.00			
	4p	−3.80	2.00			
	3d	−9.70	5.55	1.90	0.5550	0.6678
Ni[50]	4s	−7.80	2.10			
	4p	−3.70	2.10			
	3d	−9.90	5.75	2.00	0.5683	0.6292
Cu	4s	−7.80	2.20			
	4p	−3.46	2.20			
	3d	−10.00	5.95	2.30	0.5933	0.5744
H[56]	1s	−13.60	1.30			

Appendix

All calculations presented in this paper have been performed using the tight-binding formalism[48,57,58] within an extended Hückel[55,56] framework. The atomic parameters used in the calculations are listed in Table I. Extended Hückel parameters for all metals except Sc, Ti, and Cu have been obtained by charge iteration on metallic slabs.[50] The values for Sc, Ti, and Cu have been adjusted to reproduce the band widths and Fermi-level positions shown in Figure 3. The general trends reproduced in Figure 3 agree with the results of calculations performed with other computational methods.[86]

A set of 30k points in the 2D hexagonal Brillouin zone was used for the calculation of average properties on the (0001) type interfaces. A 36k point set in the 2D rectangular Brillouin zones was used for the (10$\bar{1}$0) and (1$\bar{1}$02) interfaces. Both sets of special K points were obtained using the geometric method described by Ramírez and Böhm.[100] The geometrical parameters of the metal slabs in our calculations are given in Table II.

References and Notes

(1) *Metal-Support Interactions in Catalysis, Sintering and Redispersion*; Stevenson, S. A., Dumesic, J. A., Baker, R. T. K., Ruckenstein, E., Eds.; Van Nostrand Reinhold: New York, 1987.
(2) Humerik, Jr., M.; Kingery, W. D. *J. Am. Chem. Soc.* **1954**, *37*, 18.
(3) Humerik, Jr., M.; Whalen, I. J. In *Cerments*; Tinklepaugh, J. R., Crandall, W. B., Eds.; New York, 1960; pp 6–49.
(4) McDonald, J. E.; Eberhart, J. G. *Trans. Metal. Soc. AIME* **1965**, *233*, 512–517.

(5) de Bruin, H. J. In *Surface and Near-Surface Chemistry of Oxide Materials*; Nowotny, J.; Dufour, L.-C.; Elsevier: Amsterdam, 1988; pp 507–527.
(6) Klomp, J. T. In *Ceramic Microstructures '86*; Pask, J. A., Evans, A. G., Eds.; Plenum: New York, 1987; pp 307–317.
(7) Loehman, R. E. *Am. Ceram. Soc. Bull.* **1989**, *68*, 891.
(8) Peirce Jr., R. W.; Vaughan, J. G. In *IEEE Transactions on Components, Hybrids and Manufacturing Technology*; CHMT, 1983; p 202.
(9) Torkington, R. S.; Vaughan, J. G. *J. Vac. Sci. Technol.* **1985**, *A3*, 795.
(10) Vaughan, J. G.; Zawicki, L. R.; Thomas, N. C. *J. Vac. Sci. Technol.* **1982**, *20*, 383.
(11) Baglin, J. E. E.; Clark, G. J.; Bøttiger, J. In *Thin Films and Interfaces*; Baglin, J. E., Campbell, D. R., Chu, W. K., Eds.; Elsevier: Amsterdam, 1984; p 205.
(12) Bøttiger, J.; Baglin, J. E. E.; Brusic, V.; Clark, G. J.; Anfiteatro, D. In *Thin Films and Interfaces*; Baglin, J. E., Campbell, D. R., Chu, W. K., Eds.; Elsevier: Amsterdam, 1984; p 205.
(13) Mulder, C. A. M.; Klomp, J. T. *J. Phys.* **1985**, *C4*, 111.
(14) Backhaus-Ricoult, M. *Ber. Bunsen-Ges. Phys. Chem.* **1987**, *90*, 684.
(15) Heinrich, V. E. In *Surface and Near-Surface Chemistry of Oxide Materials*; Nowotny, J., Dufour, L.-C., Eds.; Elsevier: Amsterdam, 1988; pp 23–57.
(16) Derby, B.; Wallach, E. R. *J. Mater. Sci.* **1982**, *15*, 49.
(17) Derby, B.; Wallach, E. R. *J. Mater. Sci.* **1984**, *18*, 427.
(18) Stoneham, A. M.; Tasker, P. W. In *Surface and Near-Surface Chemistry of Oxide Materials*; Nowotny, J., Dufour, L.-C., Eds.; Elsevier: Amsterdam, 1988; pp 1–20.
(19) Hofmann, S. *J. Chim. Phys.* **1987**, *84*, 141.
(20) Hondros, E. D. In *Techniques of Metals Research Series*; Rapp, R. A., Ed.; Wiley-Interscience: New York, 1970; pp 293–348.
(21) Fischmeister, H. F.; Navara, E.; Easterling, K. E. *Met. Sci. J.* **1972**, *6*, 211.
(22) Fecht, H. J.; Lojkowski, W.; Gleiter, H. *J. Phys.* **1985**, *C4*, 107–109.
(23) Li, J.-G. *J. Am. Ceram. Soc.* **1992**, *75*, 3118–26.
(24) Stoneham, A. M.; Tasker, P. W. *Philos. Mag. B* **1987**, *55*, 237–252.
(25) Anderson, A. B.; Mehandru, S. P.; Smialek, J. L. *J. Electrochem. Soc.* **1985**, *132*, 1695–1701.
(26) Anderson, A. B.; Ravimohan, C.; Mehandru, S. P. *Surf. Sci.* **1987**, *183*, 438–448.
(27) Nath, K.; Anderson, A. B. *Phys. Rev. B* **1988**, *38*, 8264.
(28) Nath, K.; Anderson, A. B. *Phys. Rev. B* **1989**, *39*, 1013–1019.
(29) Johnson, K. H.; Pepper, S. V. *J. Appl. Phys.* **1982**, *53*, 6634–6637.
(30) Louie, S. G.; Cohen, M. L. *Phys. Rev. B* **1976**, *13*, 2461.
(31) Louie, S. G.; Chelikowsky, J. G.; Cohen, M. L. *Phys. Rev. B* **1977**, *15*, 2154.
(32) Van de Walle, C. G.; Martin, R. M. *J. Vac. Sci. Technol. B* **1985**, *3*, 1256.
(33) Zdetsis, A. D.; Kunz, A. B. *Phys. Rev. B* **1985**, *32*, 6358–6362.
(34) Kunc, K.; Martin, R. M. *Phys. Rev. B* **1981**, *13*, 3445.
(35) Hong, S. Y.; Anderson, A. B.; Smialek, J. L. *Surf. Sci.* **1990**, *230*, 175–183.
(36) Ohuchi, F. S.; French, R. H.; Kasowski, R. V. *J. Appl. Phys.* **1987**, *62*, 2286–2289.
(37) Kasowski, R. V.; Ohuchi, F. S. *Phys. Rev. B* **1987**, *35*, 9311–9313.
(38) Kasowski, R. V.; Ohuchi, F. S.; French, R. H. *Physica B* **1988**, *150*, 44–46.
(39) Kohyama, M.; Kose, S.; Kinoshita, M.; Yamamoto, R. *J. Phys. Chem. Solids* **1992**, *53*, 345–354.
(40) Klomp, J. T.; Vrugt, P. J. In *Surfaces and Interfaces in Ceramic and Metal–Ceramic Systems*; Pask, J. A., Evans, A. G., Eds.; Plenum: New York, 1981; p 97.
(41) Klomp, J. T. In *Ceramic Surfaces and Surface Treatments*; Morrell, R., Nicholas, M. G., Eds.; Shelton House: Stoke-on-Trent, 1984; pp 249–259.
(42) Klomp, J. T. In *Electronic Packaging Materials Science*; Giess, E. A., Tu, K., Uhlmann, D. R., Eds.; MRS: Pittsburgh, 1985; pp 281–291.
(43) Lee, L. H. In *Fundamentals of Adhesion*; Lee, L. H., Ed.; Plenum: New York, 1990.
(44) Rühle, M.; Evans, A. G. *Mater. Sci. Eng.* **1989**, *A107*, 187.
(45) *Metallization and Metal-Semiconductor Interfaces*; Batra, I. P., Ed.; Plenum: New York, 1989.
(46) Alemany, P.; Boorse, R. S.; Burlitch, J. M.; Hoffmann, R. *Chem. Mater.* **1993**, *5*, 465–471.
(47) Hoffmann, R. *Solids and Surfaces: A Chemist's View of Bonding in Extended Structures*; VCH Publishers: New York, 1988.
(48) Ashcroft, N. W.; Mermin, N. D. *Solid State Physics*; Holt, Rinehart and Winston: New York, 1976.
(49) Zangwill, A. *Physics at Surfaces*; Cambridge University Press: Cambridge, 1988.
(50) Saillard, J.-Y.; Hoffmann, R. *J. Am. Chem. Soc.* **1984**, *106*, 2006–2026.
(51) Elliot, S. R. *Physics of Amorphous Materials*; Longman: Birmingham, AL, 1990.
(52) Joannopoulos, J. D.; Cohen, M. L. *Phys. Rev. B* **1973**, *7*, 2644–2657.
(53) Joannopoulos, J. D. *Phys. Rev. B.* **1977**, *16*, 2764.
(54) Joannopoulos, J. D. *J. Non-Cryst. Solids* **1979**, *32*, 241–255.
(55) Hoffmann, R.; Lipscomb, W. N. *J. Chem. Phys.* **1962**, *36*, 2176–2195.
(56) Hoffmann, R. *J. Chem. Phys.* **1963**, *39*, 1397–1412.
(57) Whangbo, M.-H.; Hoffmann, R. *J. Am. Chem. Soc.* **1978**, *100*, 6093.

(58) Whangbo, M.-H.; Hoffmann, R.; Woodward, R. B. *Proc. R. London, A* **1979**, *366*, 23.

(59) Albright, T. A.; Burdett, J. K.; Whangbo, M. H. *Orbital Interactions in Chemistry*; John Wiley & Sons: New York, 1985.

(60) Pauling, L.; Hendricks, S. B. *J. Am. Chem. Soc.* **1925**, *47*, 781–790.

(61) Newham, R. E.; De Haan, Y. M. *Z. Kristallogr.* **1962**, *117*, 235–237.

(62) Guo, J.; Ellis, D. E.; Lam, D. *J. Phys. Rev. B* **1992**, *45*, 13647–13656.

(63) Mayer, J.; Gutekunst, G.; Möbus, G.; Dura, J.; Flynn, C. P.; Rühle, M. *Acta Met. Mater.* **1992**, *40*, s217–s225.

(64) Pearson, W. B. *Handbook of Lattice Spacings of Metals and Alloys*; Pergamon: New York, 1958.

(65) Arakawa, E. T.; Williams, M. W. *J. Phys. Chem. Solids* **1968**, *29*, 735.

(66) Balzarotti, A.; Bianconi, A.; Burattini, E.; Grandolfo, M.; Habel, R.; Piacentini, M. *Phys. Status Solidi* **1974**, *63*, 77.

(67) Brytov, I. A.; Romashchenko, Y. N. *Fiz. Tverd. Tela (Leningrad)* **1978**, *20*, 664.

(68) Codling, K.; Madden, R. P. *Phys. Rev.* **1968**, *167*, 587.

(69) Fomichev, V. A. *Fiz. Tverd. Tela (Leningrad)* **1966**, *8*, 2892.

(70) Fisher, D. W. *Adv. X-ray Anal.* **1970**, *13*, 159.

(71) Balzarotti, A.; Bianconi, A. *Phys. Status Solidi B* **1976**, *76*, 689.

(72) Kowalczyk, S. P.; McFeely, F. R.; Ley, L.; Gritsyna, V. T.; Shirley, D. A. *Solid State Commun.* **1977**, *23*, 161.

(73) Olivier, J.; Poirier, R. *Surf. Sci.* **1981**, *105*, 347.

(74) Reilly, M. H. *J. Phys. Chem. Solids* **1970**, *31*, 1041.

(75) Brower, K. L. *J. Vac. Sci. Technol.* **1975**, *12*, 458.

(76) Tossel, J. A. *J. Am. Chem. Soc.* **1975**, *97*, 4840.

(77) Tossel, J. A. *J. Phys. Chem. Solids* **1975**, *36*, 1273.

(78) Shangda, X.; Chanxin, G.; Libin, L.; Ellis, D. E. *Phys. Rev. B* **1987**, *35*, 7671.

(79) Evarestov, R. A.; Ermoshkin, A. N.; Lovchikov, V. A. *Phys. Status Solidi B* **1980**, *99*, 387.

(80) Batra, I. P. *J. Phys. C* **1982**, *15*, 5399.

(81) Ciraci, S.; Batra, I. P. *Phys. Rev. B* **1983**, *28*, 982–992.

(82) Causà, M.; Dovesi, R.; Roetti, C.; Kotomin, E.; Saunders, V. R. *Chem. Phys. Lett.* **1987**, *140*, 120–123.

(83) Causà, M.; Dovesi, R.; Pisani, C.; Roetti, C. *Surf. Sci.* **1989**, *215*, 259–271.

(84) Guo, J.; Ellis, D. E.; Lam, D. *J. Phys. Rev. B* **1992**, *45*, 320.

(85) Il'mas, E. R.; Kuznetsov, A. I. *Fiz. Tverd. Tela (Leningrad)* **1972**, *14*, 1464.

(86) Papaconstantopoulos, D. A. *Handbook of The Band Structure of Elemental Solids*; Plenum Press: New York, 1986.

(87) Andersen, O. K. In *The Electronic Structure of Complex Systems*; Phariseau, P., Temmerman, W. M., Eds.; Plenum Press: New York, 1984.

(88) Andersen, O. K. In *Highlights of Condensed Matter Physics*; Bassani, F., Fumi, F., Tossi, M. P., Eds.; North-Holland, New York, 1984.

(89) Zheng, C.; Apeloig, Y.; Hoffmann, R. *J. Am. Chem. Soc.* **1988**, *110*, 749–774.

(90) French, T. M.; Somorjai, G. A. *J. Phys. Chem.* **1970**, *74*, 2489–2495.

(91) Chang, C. C. *J. Appl. Phys.* **1968**, *39*, 5570–5573.

(92) Charig, J. M. *Appl. Phys. Lett.* **1967**, *10*, 139.

(93) Susnitzky, D. W.; Carter, C. B. *J. Am. Ceram. Soc.* **1986**, *69*, C-217.

(94) Baik, S.; Fowler, D. E.; Balkely, J. M.; Raj, R. *J. Am. Chem. Soc.* **1985**, *68*, 281.

(95) Peden, C. H. F.; Kidd, K. B.; Shinn, N. D. *J. Vac. Sci. Technol. A* **1991**, *9*, 1518–1524.

(96) Morozumi, S.; Kikuchi, M.; Nishino, T. *J. Mater. Sci.* **1981**, *16*, 2137–2144.

(97) Ealet, B.; Gillet, E. *Surf. Sci.* **1993**, *281*, 91–101.

(98) Gillet, E.; Legressus, C.; Gillet, M. *J. Chim. Phys.* **1987**, *84*, 167–174.

(99) Gignac, W. J.; Williams, R. S.; Kowalczyk, S. P. *Phys. Rev. B* **1985**, *32*, 1237.

(100) Ramírez, R.; Böhm, M. C. *Int. J. Quantum Chem.* **1986**, *30*, 391.

(101) Anderson, A. B.; Hoffmann, R. *J. Chem. Phys.* **1974**, *60*, 4271.